# Region-Based Phasor Analysis of Multispectral Retinal Images for Disease Identification

**Armin Eskandarinasab*, Laura Rey-Barroso, Francisco J. Burgos-Fernández, Meritxell Vilaseca**

*Center for Sensors, Instruments and Systems Development, Universitat Politècnica de Catalunya, Rambla Sant Nebridi 10, Terrassa, 08222, Spain*
*#corresponding author email: armin.eskandarinasab@upc.edu*
**presenting author*

## 1. Introduction

Multispectral cameras are a valuable tool for ophthalmologists to diagnose eye diseases. Unlike standard cameras, which capture images in RGB format, they can capture images across a wide range of wavelengths. This allows them to gather detailed information about the retina. However, multispectral cameras also capture a large amount of data corresponding to multiple bands, often more than 10 spanning from infrared to visible and even ultraviolet, which can be challenging to process.

The large amount of data collected by multispectral cameras presents both opportunities and challenges. On the one hand, it provides a rich source of information that can be valuable for diagnosis and analysis. On the other hand, the massive amount of data can lead to redundancy and make it difficult to process and interpret, whether by humans or machine learning algorithms.

To overcome this challenge, it is essential to reduce the dimensionality of the data without sacrificing important information. One approach to achieving this is through dimensionality reduction methods such as phasor analysis, which can help extracting the essential features from the data and make it more manageable. For instance, in [1], phasor analysis was employed to enhance the accuracy of classification algorithms, such as $\nu$-SVM, in distinguishing between healthy and diseased retinas. Similarly, in [2], phasor analysis was used to re-color images, effectively reducing their dimensionality and making them more interpretable for human analysis.

In these analyses, the phasor technique was applied to the entire retinal region. In contrast, this study proposes a more nuanced approach, where specific regions of interest are considered separately, including the optic disk, macula, vessels, and background. By analyzing each region individually, we can gain a more detailed understanding of their characteristics between healthy and diseased cases.

## 2. Materials, methods and results

The multispectral images were captured using a custom-built fundus camera [3]. This camera employs an array of LEDs, each emitting light at a distinct peak wavelength. The camera's high-resolution CMOS sensor, with 2048 $\times$ 2048 pixels and a 6.5 µm pixel size, captures 12 spectral images across a range of 416 to 955 nm. The sensor's 16-bit depth provides high dynamic range and detailed image data. After processing and cropping, the images were reduced to 1757 $\times$ 1757 pixels.

This study utilized a dataset of 40 multispectral retinal images, which included 21 cases of diseased retinas and 19 healthy controls. The diseased retinas captured a variety of conditions, such as Age-related Macular Degeneration (AMD), epiretinal membrane, glaucoma, and retinal detachment, as well as other retinal pathologies. The images were sourced from two esteemed ophthalmic centers: the Instituto de Microcirugia Ocular (IMO - Miranza Group) in Barcelona, Spain, and the Vision University Center (CUV) of the Universitat Politècnica de Catalunya in Terrassa, Spain [4].

To have region-specific analysis of the retina, image masks were employed to isolate areas of interest. Manual creation of masks was performed for four distinct regions: the optic disk, macula, vessels, and background. An example of a multispectral image and its corresponding masks is provided in Fig.1. Nextly, phasor analysis was computed for each pixel in the spectral cube ($x$, $y$, $\lambda$), resulting a complex number for each pixel ($g_{x,y} + is_{x,y}$) processed via discrete Fourier transform [5, 6].

$$g_{x,y}(k) = \frac{\sum_{\lambda_0}^{\lambda_n} I_{x,y}(\lambda) * \cos(\frac{2\pi k\lambda}{2}) * \Delta\lambda}{\sum_{\lambda_0}^{\lambda_n} I_{x,y}(\lambda) * \Delta\lambda}, s_{x,y}(k) = \frac{\sum_{\lambda_0}^{\lambda_n} I_{x,y}(\lambda) * \sin(\frac{2\pi k\lambda}{2}) * \Delta\lambda}{\sum_{\lambda_0}^{\lambda_n} I_{x,y}(\lambda) * \Delta\lambda}$$

Where $\lambda_0$ and $\lambda_n$ are the first and last wavelengths of the spectral channels which mean from the first to the last wavelength are involved in calculation of each $g_{x,y}$ and $s_{x,y}$. Besides that, $n$ is the number of spectral channels, $\Delta\lambda$ is the spectral bandwidth, and $k$ is the harmonic number.

Fig. 1. Example of a multispectral image and its corresponding masks for different regions of the retina. From left to right: multispectral image, vessels mask, optic disk mask, macula mask, and background mask.

Each multispectral image was encoded into $g_{x,y}$ and $s_{x,y}$ components, and then averaged to get a single vector $(g_{avg}, s_{avg})$ per image. The averaged phasor values for each retinal region analyzed are shown in Fig.2. Additionally, after comparing different harmonics, the first harmonic (k=1) showed the maximum separation between healthy and diseased cases in comparison to the other ones. In the plots, the standard deviation of phasor values represents the radius of each point.

Fig.2 shows a clear separation between healthy and diseased cases across all regions. The size of the circles, representing the standard deviation of phasor values, varies between regions and disease states. The background and vessels regions show similar circle sizes for both healthy and diseased cases, whereas the macula and optic disk regions display larger variations in circle size, particularly for diseased cases. Further analysis revealed that circle size is correlated with disease severity and type. For instance, in glaucoma cases, the optic disk region's circle size is larger than in other diseased cases, likely due to the region's specific involvement in the disease. Similarly, in the macula region, the largest circle indicates a case where the macula area in the patient's eye has a significant scar.

Therefore, the standard deviation of phasor values can serve as a potential biomarker for detecting region-specific diseases, allowing for the identification of abnormalities in the macula and optic disk regions that may be associated with various retinal conditions.

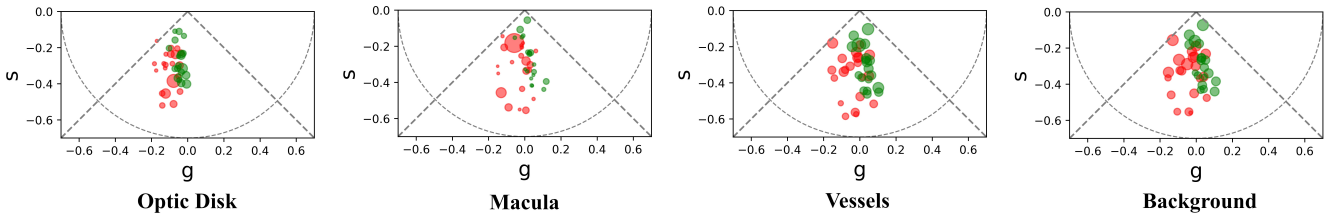


Fig. 2. Averaged phasor values for different regions of the retina using the first harmonic. Each point represents the average phasor value for a specific region, with the radius indicating the standard deviation of the phasor values within that region. The color coding is as follows: green for healthy cases, and red for diseased cases.

## 3. Acknowledgment

Funded by European Union (HORIZON–MSCA–2022–DN, GA nº101119924–BE-LIGHT) and by MCIU /AEI /10.13039/501100011033 and FEDER, EU (Grant PID2023-147541OB-I00).

## 4. References

[1] Eskandarinasab, A., et al. "Exploiting Spectral Signatures for Retinal Health Assessment: A Phasor Analysis Approach" in European Conference on Biomedical Optics (ECBO) 2025, Munich, Germany, (2025), Conference Presentation.

[2] Eskandarinasab, A., et al. "Color-Coded Phasor Analysis for Improved Retinal Disease Differentiation," in XIV Congreso Nacional del Color, Mérida, Spain, (2025), Conference Presentation.

[3] Alterini, T., et al. "Fast Visible and Extended Nnear-Infrared Multispectral Fundus Camera," Journal of Biomedical Optics, 24(9), 096007-096007# (2019).

[4] Burgos-Fernández, F.J., et al, "Reflectance Evaluation of Eye Fundus Structures with a Visible and Near-Infrared Multispectral Camera," Biomedical Optics Express, 13(6), 3504-3519# (2022).

[5] Malacrida, L., et al, "Model-free methods to study membrane environmental probes: a comparison of the spectral phasor and generalized polarization approaches," Methods and Applications in Fluorescence, 3(4), 047001# (2015).

[6] Cutrale, F., et al, "Hyperspectral Phasor Analysis Enables Multiplexed 5D in vivo Imaging," Nature methods, 14(2), 149-152# (2017).